Timing of human-induced climate change emergence from internal climate variability for hydrological impact studies

Mei-Jia Zhuan[1], Jie Chen[1*], Ming-Xi Shen[1], Chong-Yu Xu[1, 2], Hua Chen[1], Li-Hua Xiong[1]

[1] State Key Laboratory of Water Resources and Hydropower Engineering Science, Wuhan University, Wuhan 430072, P. R. China

[2] Department of Geosciences, University of Oslo, PO box 1047 Blindern, N-0316 Oslo, Norway

*corresponding author, Email: jiechen@whu.edu.cn; Phone: +86-17764063119

Abstract: This study proposes a method to estimate the timing of human-induced climate change (HICC) emergence from internal climate variability (ICV) for hydrological impact studies based on climate model ensembles. Specifically, ICV is defined as the inter-member difference in a multi-member ensemble of a climate model in which human-induced climate trends have been removed through a detrending method. HICC is defined as the mean of multiple climate models. The intersection between HICC and ICV curves is defined as the time of emergence (ToE) of HICC from ICV. A case study of the Hanjiang River watershed in China shows that the temperature change has already emerged from ICV during the last century. However, the precipitation change will be masked by ICV up to the middle of this century. With the joint contributions of temperature and precipitation, the ToE of streamflow occurs about one decade later than that of precipitation. This implies that consideration for water resource vulnerability to climate should be more concerned with adaptation to ICV in the near-term climate (present through mid-century), and with HICC in the long-term future, thus allowing for more robust adaptation strategies to water transfer projects in China.

Key words: Climate change impacts, Human-induced climate change, Internal climate variability, Time of emergence, Hydrology

INTRODUCTION

The Intergovernmental Panel on Climate Change (IPCC, 2014) states that consecutive changes of precipitation pattern and temperature will give rise to a wide scope of environmental and socio-economic impacts by the end of the 21st century. Global climate change is driven on all timescales beyond that of individual weather events by internal and external forcing (IPCC, 2014). Internal forcing includes naturally occurring processes in ocean and atmosphere, and interactions of ocean and atmosphere within the climate system. Internal forcing exists as far back as pre-industrial time, when the climate system was more likely in an idealized state of climatic equilibrium with a fixed atmospheric composition and an unchanging sun (IPCC, 2014). It gives rise to internal climate variability which contributes to variations in climate. In this way, internal climate variability is natural fluctuations superimposed on a stable average climate state in pre-industrial time or a human-induced climate change trend in industrial time. Variations in climate may also result from external forcing of the climate system. External forcing consists of anthropogenic forcing, such as greenhouse gas emissions and disruptive land use, and natural external forcing, such as volcanic eruptions and solar variations. The impact of volcanic eruptions generally lasts for less than a decade (IPCC, 2014), while solar variations take place at multi-decadal, multi-centennial and millennial scales (Helama et al., 2010), which are considerably longer than decades. However, the classical period for estimating climate change is 30 years, as defined by the World Meteorological Organization (IPCC, 2014). Regardless of climate change

due to natural forcing with quite different timescales (a few years for volcanic eruptions and tens of thousands of years for solar radiation (Milankovitch cycles)), climate change mainly consists of human-induced climate change (HICC) and internal climate variability (ICV).

Climate change impacts have been given much attention in recent literature, among which the importance of ICV has been discussed in several studies. For example, Deser et al. (2012b) suggested presenting the role of ICV in overall climate change on timescales of a few decades. Fyfe et al. (2013) claimed that ICV could help explain the fact that recent observed global warming is significantly less than that simulated by climate models. Swart et al. (2015) found that ICV can obscure or strengthen anthropogenic sea-ice loss at annual, decadal and multi-decadal timescales and should be properly considered in order to interpret projections and evaluate models. Fyfe et al. (2016) support the view that the effects of ICV imposed on HICC have contributed to the global surface warming slowdown or hiatus. In addition, Dai et al. (2015) concluded that ICV, mainly manifested in Interdecadal Pacific Oscillation, was largely responsible for recent global warming slowdown, as well as for earlier slowdowns and accelerations in global-mean temperature, with preferred spatial patterns different from those associated with human-induced warming or aerosol-induced cooling.

One of the other aspects of studying ICV is to investigate its contribution to the uncertainty of climate change projections. For example, Hawkins and Sutton (2009) quantified the relative contribution of ICV to the uncertainty of global temperature projections over the 21st century, using the Coupled Model Intercomparison Project

Phase 3 (CMIP3) archive. They found that ICV contributed significantly to the uncertainty of inter-decadal temperature before 2010. A follow-up study by Hawkins and Sutton (2011) for precipitation at a regional scale showed that ICV was the dominant source of uncertainty for decadal changes of precipitation in the first few decades of the 21st century. Deser et al. (2012a) investigated the uncertainty in climate change projections (surface air temperature, precipitation and sea level pressure) arising from ICV, using a 40-member ensemble of the National Center for Atmospheric Research Community Climate System Model Version 3 (CCSM3) under the A1B greenhouse gas emission scenario. Their results showed that ICV accounts for at least half of the inter-model uncertainty in projected climate (surface air temperature, precipitation and sea level pressure) trends during 2005-2060. Deser et al. (2014) also examined the contribution of ICV to the uncertainty in projected surface air temperature and precipitation trends during 2010-2060 at local and regional scales over North America from large ensembles of simulations with two comprehensive climate models, the CCSM3 and the European Centre Hamburg Model 5 (ECHAM5)-Max Planck Institute Ocean Model (MPI-OM). This study showed that ICV has significant impact on precipitation trends, and that intrinsic atmospheric circulation variability is mainly responsible for the uncertainty in future climate trends.

In addition to investigating the role and contribution of ICV in climate projection, a few studies have also quantified the magnitude of ICV relative to HICC in overall climate change using Time of Emergence (ToE) as a criterion. ToE is defined as the timing of when the magnitude of HICC becomes greater than the noise of ICV

(Hawkins and Sutton, 2012). For example, Giorgi and Bi (2009) defined HICC as the mean precipitation change over models with multiple projections, and ToE as the time when HICC emerges from a combination of inter-model variability and ICV for precipitation. Inter-model variability is defined as a variance of individual model change time series after averaging over the projections within each model. Regarding ICV itself, different changes between each simulation and the ensemble mean were obtained. Mahlstein et al. (2011) estimated HICC using the multi-model mean of summer average surface temperature. Model data were first linearly detrended, and then summer average surface temperatures were determined for each year. ICV was defined as ±2 standard deviations of summer average surface temperature after detrending. Hawkins and Sutton (2012) assumed that HICC of global mean surface air temperature follows a nonlinear trend. Thus, a 4th-order polynomial was used to fit the annual temperature. ICV was defined as the inter-annual standard deviation of seasonal (or annual) mean temperatures, using pre-industrial control simulations assumed without anthropogenic forcing. Their study implies that ToE is a basic property of climate system; the true values of which are unknown but which can be estimated using model simulations. Similarly, Maraun (2013) defined HICC as the multi-model mean of precipitation. Model data were first linearly detrended by a parametric trend model, and then ICV was defined as the inter-annual variability measured by the standard deviation of the detrended model data.

Even though the magnitude of ICV relative to HICC has been investigated in some studies, far fewer studies have discerned the timing of HICC's departure from ICV for

hydrological climate change impact studies. For example, Leng et al. (2016) detected the emergence of hydrologic changes in surface water resources in the conterminous United States under future warming. They used a two-sample Kolmogorov–Smirnov test to compare the probability distribution functions of historical and future streamflows. The emergence of significant changes is defined as the time when the future distribution differs significantly from the reference period, and when the distributions in all subsequent 30-year periods also differ significantly from the reference period. This study did not separately estimate HICC and ICV to find ToE.

Moreover, since ICV manifests itself at various temporal and spatial scales, there are many modes of ICV for climate system. Hawkins and Sutton (2012) and Maraun (2013) investigated inter-annual variability and defined the ToE of climate change signal as a specific year. While others (e.g. Giorgi and Bi, 2009; Mahlstein et al., 2011; Leng et al., 2016) investigated multi-decadal variability and defined the ToE as a period of 20 or 30 years. Since climate change impact studies are commonly conducted for multi-year periods (e.g., of 30 years) (IPCC, 2014), it may be more reasonable to estimate ICV at a multi-decadal time scale when the goal is to investigate the role of ICV in climate change impact studies. In addition, ToE estimated for a multi-year period may be more reliable and credible, since inter-annual variability is mostly smoothed by calculating the multi-year average.

The main objective of this study is to propose a method to estimate the timing of climate change emergence from ICV for hydrological impact studies based on a multi-member ensemble of a climate model. Hanjiang River watershed above the

Danjiangkou reservoir (in China) is selected to exemplify the proposed method.

STUDY AREA AND DATA

Study area

The Hanjiang River has a mainstream river length of 1577 km and a drainage area of 159,000 km^2 (figure 1). It is one of the longest tributary rivers of the Yangtze River. In the Hanjiang River watershed (a subtropical monsoon region), average annual precipitation varies from 700 mm to 1100 mm (Wang et al., 2014), mainly due to southeastern and southwestern maritime monsoons. Three quarters of the total precipitation falls from June to October, usually giving rise to great floods (Xu et al., 2012). According to hydrological regimes (e.g. Chen et al., 2012; Yang et al., 2016), May to October are considered as the wet season and the other months are considered to be the dry season. Average annual temperature is 15.5 °C. Mean annual discharge of the Hanjiang River is about 1150 m^3/s (Wang et al., 2015).

The watershed above the Danjiangkou reservoir, with a drainage area of about 89,540 km^2, is used in this study. Located in the middle and upper reaches of the Hanjiang River watershed, the Danjiangkou reservoir is the water source for the Middle Route Project of the South-to-North Water Diversion Project (Yang and Zehnder, 2005; Chen et al., 2007). In December 2014, it began to provide water for people in 20 large and medium cities in 4 provinces/municipalities, including the capital (Beijing). It also provides comprehensive benefits such as flood control, power generation, irrigation, shipping, livestock farming, tourism, and so on. The assessment of climate change

impacts on hydrology is therefore of great importance for water resource managers.

Data

This study uses both observed and model-simulated climate data. Observed data include precipitation, maximum and minimum temperatures at daily scale over 1971-2000 derived from 11 meteorological stations in the study region. Observed meteorological data were provided by the China Meteorological Data Sharing Service System. To run a lumped hydrological model, meteorological data from the 11 stations were averaged to areal mean time series using the Thiessen polygons method. The inflow to the Danjiangkou Reservoir over 1961-2000 was provided by the Bureau of Hydrology of the Changjiang Water Resources Commission in China. The reservoir inflow was calculated using a water mass balance method (e.g. Chow et al., 1988; Fenton, 1992; Deng et al., 2014). Specifically, it was calculated by adding a change of the Danjiangkou reservoir storage to the outflow at the Danjiangkou reservoir.

Climate model data used in the study include 29 global climate model (GCM) simulations obtained from the Coupled Model Intercomparison Project Phase 5 (CMIP5) and a 40-member ensemble from the Community Earth System Model version 1 (CESM1) (Table 1). All 40 members of CESM1 are simulated by one climate model under the same external forcing, but with different initial conditions. In other words, differences among 40 members are only due to internal forcing in the climate model. Therefore, the differences among 40 members in the climate model naturally represent internal climate variability in the virtual world. Multi-member ensembles (e.g. CESM1)

from Community Earth System Model (CESM) were developed to study the role of ICV in climate change impact studies (e.g. Hu and Deser, 2013; Kang et al., 2013; Lu et al., 2014; Kay et al., 2015; Fasullo and Nerem, 2016). Multi-member ensembles from CESM were verified in terms of estimating the internal precipitation and temperature variability at the multi-decadal scale at the global scale and showed a reasonable performance (e.g. Otto-Bliesner et al., 2015; Ricke and Caldeira, 2014; Kay et al., 2015). All climate model simulations cover the 1970-2100 period. The historical period is driven by historical climate forcing and the future period is driven by Representative Concentration Pathway (RCP) 8.5 forcing. The RCP8.5 implies the greatest HICC, and tends to result in the greatest rise in both climate projections and hydrological impacts.

METHODOLOGY

To estimate the timing of when HICC emerges from ICV for hydrological climate change impacts, HICC and ICV need to be estimated. HICC is defined as the ensemble mean of 29 GCM simulations and the first member of CESM1 (a mean of 30 simulations) after bias correction. For estimating ICV, a detrending method is used to remove human-induced climate trend, and then the remainder is used to calculate ICV. Since climate model simulations are usually too biased to be used as direct inputs to a hydrological model, a bias correction is used to reduce their biases. More specifically, a traditional two-step (bias correction and hydrological simulation) modeling chain is applied when assessing the climate change impact on hydrology. To assess the impacts of ICV on hydrology, one more step (detrending) is added in the modeling chain to

remove climate trend from the CESM1 ensemble. The other two steps are the same. More details are given below.

Detrending methods

A two-stage detrending method was used to remove climate trend from the CESM1 ensemble. The climate trend is assumed to follow a linear trend. Since all CESM1 members are simulated using the same model structure and driven by identical climate forcing, it is expected that all members include the same climate trend. Thus, the climate trend is estimated based on a 40-member ensemble mean.

Since the CESM1 simulations are driven by different forcings during the historical period (1970-2005) and the future period (2006-2100), the climate trend may be different between these two periods. Thus, a two-stage method is used to detect and remove trends of climate change for the two periods separately. For each period, a Mann-Kendall test is used to discern if a significant trend exists. In the first stage, if a significant trend exists in the historical period, the Mann-Kendall test is further used to find a breakpoint that separates the historical period into sub-periods with and without a climate trend. In other words, the first sub-period is free of human-induced climate trend, while the detected trend begins at the breakpoint and extends throughout the second sub-period. Since several breakpoints may exist when using the Mann-Kendall test, the sum of squared errors (SSE) is used as a criterion to find the real breakpoint, which can best distinguish the two sub-periods. The SSE of prediction is calculated based on the mean value over the first sub-period and the fitted linear trend over the

second sub-period. To detrend the climate trend for the historical period, the first sub-period is assumed to be unchanged, while a linear curve is fitted to the second sub-period with its first point forced to pass through the mean of the first sub-period; that same trend is then removed from each of the 40 members. In the second stage if a significant trend exists for the future period, a linear curve is fitted to the ensemble mean of 40 members. The same trend is then removed from each of the 40 members. The difference between the mean values of the historical and future periods is removed in the last step. The observed precipitation and mean temperature may also contain climate trends. If the Mann-Kendall test shows a significant trend, the first stage of the above method is used to remove the climate trend for the single time series. ICV is the residual of the data after the trend removal step.

Bias correction

A quantile mapping bias correction was used to correct the bias for a multi-member ensemble of CESM1 and 29 climate model simulations. This method (Schmidli et al., 2006; Mpelasoka and Chiew, 2009; Chen et al., 2013) is a combination of the Daily Transition (DT) (Mpelasoka and Chiew, 2009) and Local Intensity Scaling (LOCI) (Schmidli et al., 2006; Chen et al., 2011b) methods, and is known as daily bias correction (DBC) in Chen et al. (2013). The LOCI method is first used to correct precipitation occurrence, insuring that the frequency of precipitation occurrence of corrected data at the reference period is equal to that of observed data for each month. Next, the DT method is applied to correct the frequency distribution of precipitation

amounts and temperatures based on quantile differences between model data and observed data.

The DBC method was calibrated at a historical period (1971-2000) and applied to multiple 30-year periods. The multiple periods are sliding 30-year time windows that vary by one year, e.g. 1970-1999, 1971-2000, 1972-2001, etc., over the whole period (1970-2100), totaling 102 periods. When correcting CESM1, all members were pooled together to estimate bias correction factors. In other words, correction factors were estimated as the difference between observed data and all the members of the model data during a reference period (1971-2000). For each of the 40 ensemble members, correction factors, assumed to be constant over time, were applied to model data for the whole period (1970-2100). All the members of CESM1 are treated as a whole because all CESM1 members were simulated using the same climate model with identical climate forcing, and therefore it is expected that all members have the same model biases. When correcting the other 29 GCM simulations, correction factors were estimated for each GCM simulation. In other words, each climate simulation was corrected individually.

Hydrological simulation

The hydrological modeling was carried out using a lumped conceptual rainfall-runoff model, HMETS, developed at the École de technologie supérieure, University of Quebec (Martel et al., 2017). HMETS has been used in a number of flow prediction and climate change impact studies (e.g. Arsenault et al., 2013; Chen et al., 2014). It accounts

for evapotranspiration, infiltration, snow accumulation, melting and refreezing processes, and flow routing to a watershed's outlet. The model has up to 21 free parameters: one for evapotranspiration, ten for snow accumulation and snowmelt, four for vertical water balance, and six for horizontal water movement. For rainfall-dominated watersheds (as is the case in this study), HMETS' snow module is not used, and so the model used in this study has 11-parameter to be determined. The required daily input data for HMETS are the daily averaged precipitation and daily mean air temperature. If the maximum and minimum temperatures are input to the model, they are automatically averaged to the mean temperature. The daily inflow discharge time series is also used for calibration (1961-1980) and validation (1981-2000) purpose.

Model calibration was done automatically using the Covariance Matrix Adaptation Evolution Strategy (CMAES) (Hansen and Ostermeier, 2001). The Nash-Sutcliffe efficiency was used for model evaluation. The chosen set of parameters yielded Nash-Sutcliffe criterion values of 0.79 and 0.78 for the calibration and validation periods, respectively. Considering the fact that climate data from only 11 meteorological stations were used in model calibration at the daily scale, the performance of HMETS is considered acceptable for the studied watershed. The mean hydrographs of the observed and simulated flows over both the calibration and validation periods are drawn in figure 2.

Estimation of the Time of Emergence

The timing of HICC emerging from ICV (time of emergence, ToE) was estimated both

for climate projections and hydrological simulations. HICC and ICV were estimated using the method described below.

The HICC is calculated with the following four steps. (1) Using the DBC method, 102 bias-corrected periods were obtained for all 30 simulations. The 102 periods are 30-year horizons varying by one year over the whole period (1970-2100), i.e. 1970-1999, 1971-2000, 1972-2001,…, 2071-2100. (2) The 30-year mean value was calculated for each period. A total of 102 mean values were obtained for each climate simulation. (3) The change (relative change for precipitation and streamflow, and absolute change for temperature) in each of 102 mean values relative to mean value at the reference period (1971-2000) was calculated. (4) The mean value of these changes over 30 simulations was defined as HICC.

The multi-decadal inter-member variability is used to represent ICV in this study. Specifically, the following four steps are involved. (1) Using the detrended and bias-corrected 40-member ensemble, 102 30-year periods were divided for each ensemble member. (2) The 30-year mean value was calculated for each period and a total of 102 mean values were obtained for each ensemble member. (3) The change (relative change for precipitation and streamflow, and absolute change for temperature) in each of the 102 mean values relative to mean value at the reference period (1971-2000) was calculated. (4) The standard deviation of these changes over 40 members was calculated for each period and a total of 102 standard deviation values were obtained. ICV was then defined as ±2 standard deviations of inter-member differences. According to the '3σ' principle of normal distribution, the chance for absolute values of climate change

(attributed to ICV) to exceed +2 standard deviations of inter-member differences is only 2.3% and the same is true for -2 standard deviations (Hansen et al., 2012). Therefore, when absolute values of climate change become greater than ±2 standard deviations of inter-member differences, the climate change is most likely to be attributed to HICC. Similar method has also been used in other studies (e.g. Hulme et al., 1999, Mahlstein et al., 2011; Hansen et al., 2012; IPCC, 2013).

With the above steps, 102 HICC values form a curve and 102 ICV values form another curve; the intersection of these two curves is defined as the ToE. If an HICC curve intersects an ICV curve of +2 standard deviations, it implies that there is an increasing climate change trend. If an HICC curve intersects an ICV curve of -2 standard deviations, then there is a decreasing climate change trend. No intersection implies that HICC does not emerge from ICV or that there is no obvious HICC. To produce conservative adaptation strategies for HICC impacts, ±1 standard deviation is also calculated. The period between the intersections of ±2 and ±1 standard deviations is defined as an unpredictable time period. The same procedure was carried out for precipitation, mean temperature and streamflow at annual and seasonal scales (wet season: May to October; dry season: January to April and November to December). The dry and wet seasons were defined based on climatic and hydrological regimes in the Hanjiang River watershed.

RESULTS

Performance of the detrending method

The detrending method was applied to mean temperature and precipitation time series over the 1971-2000 reference period for observations and over the 1970-2100 period for a CESM1 40-member ensemble. Figure 3 presents the detrending results for mean temperature and precipitation of a CESM1 40-member ensemble at annual and seasonal time scales. For this specific watershed, annual and wet season mean temperatures show little trend, while dry season mean temperature shows a significant decreasing trend for the historical period tested by the Mann-Kendall test at the p=0.05 significant level. However, annual and seasonal mean temperatures exhibit a significant increasing trend for the future period. For annual and seasonal precipitation, a significant downtrend is observed for the historical period, while a significant uptrend is observed for the future period. The detrending method performs reasonably well in terms of removing the trend of the multi-member ensemble. Residual ensemble spread represents ICV, which obviously has been preserved throughout the detrending process, since fluctuations and ensemble spread remain almost the same with raw data for the same time series.

Performance of the bias correction method

To verify the performance of bias correction in correcting multi-member ensemble, the multi-member ensemble of CESM1 mean temperature and precipitation is compared to the observed counterparts for the reference period (1971-2000). Figure 4 presents

empirical cumulative distribution functions (CDFs) of the detrended annual mean temperature and precipitation for raw and bias-corrected 40-member ensembles of CESM1. The empirical cumulative distribution function (e.g. F(x)) is defined as the ratio of the number (e.g. a) of annual mean temperatures or annual precipitations that are less than a certain value (e.g. x) and sample size (e.g. n) plus one (i.e. F(x) =a/ (n+1)). For each empirical probability, a horizontal range was constructed by 40 values corresponding to 40 members of CESM1. All members were pooled together to plot an empirical CDF curve and CDFs for observed annual mean temperature and precipitation were also plotted for comparison.

For raw model data, wet biases are observed for annual precipitation and cool biases are observed for annual mean temperature. In other words, the CESM1 ensemble underestimates annual mean temperature and overestimates annual precipitation. After bias correction, wet biases in precipitation and cool biases in mean temperature were removed, as indicated by the fact that the CDFs of corrected ensembles are almost identical to those of observed data for both mean temperature and precipitation. This result proves the good performance of bias correction in terms of removing bias from multi-member ensemble means.

In a departure from traditional studies that use single climate simulation, this study used a bias correction method for a multi-member ensemble. This approach should not only reduce the biases of climate model outputs, but also preserve the simulated ICV. ICV can be represented by a spread of 40 CDFs corresponding to 40 CESM1 members. If the bias correction was conducted for each member individually, the CDFs of all

members should be almost identical to observed CDFs. Figure 4 shows that, after bias correction, the spread of 40 ensemble members remains almost the same as those of raw model data for temperature and precipitation. This indicates the reasonable performance of the bias correction methods in terms of preserving the inter-member variability of multi-member ensembles.

Performance of hydrological simulation

Figures 5(A) and 5(B) show mean hydrographs simulated by raw and corrected climate simulations, respectively. Specifically, hydrographs were calculated by averaging daily streamflows over 30-year reference period (1971-2000) for each of 40 members. Figures 5(C) and 5(D) present empirical CDFs of annual 95th percentile high flow and annual 5th percentile low flow. The empirical CDFs of high- and low-flows were calculated as with those of precipitation and temperature in Figure 4.

The raw CESM1 ensemble considerably overestimates mean, high and low flows. The 40-member ensemble hydrograph envelope simulated by raw data is totally beyond the hydrograph simulated by observed climate data. Similar results are also observed for high- and low-flows, as empirical CDFs are all greater than counterparts of observed data. This was as expected, because the CESM1 ensemble overestimates precipitation and underestimates temperature. With bias correction, the 40-member hydrograph envelope covers the observed counterpart, and also the envelope of empirical CDFs embraces the observed counterpart for both high- and low-flows. This indicates that the model bias in climate data has been removed and so the hydrological simulation is

reliable. The variation between observed and simulated hydrographs is caused by ICV.

Times of emergence of climate change projection

Times of emergence for temperature

Figures 6(A) to 6(C) present the ToEs for annual and seasonal mean temperatures. Both annual and seasonal mean temperature HICCs display a gradually increasing pattern. For example, annual mean temperature HICC increases by 4°C from the end of the 20th century to the end of the 21st century. ICV in mean temperature is generally constant during the studied period, as indicated by the horizontal curve. In addition, ICV is small for annual and seasonal mean temperatures, as it is less than 0.5°C. Both annual and seasonal mean temperature HICCs first increase slowly and then faster, and then after a certain point they increase steadily. For example, annual mean temperature HICC increases slowly from period 1971-2000 to period 1980-2009. It then increases at a rate that gradually becomes greater until period 2017-2046; thereafter the rate of increase stays relatively constant.

Two curves intersect at the 1981-2010 period for annual mean temperature, at the 1981-2010 period for wet season mean temperature, and at the 1984-2013 period for dry season mean temperature. When using ±1 standard deviation to represent ICV, the ToE will move backwards by around 5 years.

Times of emergence for precipitation

Figures 6(D) to 6(F) present the ToE for annual and seasonal precipitations. In contrast

to mean temperature changes, annual and wet season precipitation HICCs first show a slight decreasing trend until the 2030s, and then they start gradually increasing. Dry season precipitation HICC shows a significant increasing pattern over the 1970-2100 period. Wet season precipitation HICC contributes more to annual precipitation HICC, as rainfall in the studied watershed mainly happens in the wet season. ICV is generally constant during the 1970-2100 period.

The HICC curve crosses the ICV curve at the 2043-2072 period for annual precipitation, at the 2052-2081 period for wet season precipitation and at the 2001-2030 period for dry season precipitation, respectively. When using ±1 standard deviation to represent ICV, the ToE will move backwards by about 10 years.

Time of emergence for hydrological impact

Figures 7(A) to 7(C) present the ToE for annual and seasonal mean streamflows. The results show that the human-induced change in annual and wet season mean streamflows display a slight decreasing trend until the 2030s and then they start to increase gradually. While for the dry season streamflow, the turning point is at the 2000s.

The HICC curve crosses the ICV curve at the 2055-2084 period for annual mean streamflow, at the 2056-2085 period for wet season mean streamflow, and at the 2061-2090 period for dry season mean streamflow, respectively. This indicates that the human-induced changes in annual and seasonal streamflows are likely to move out of the range of the internal streamflow variability in the second half of the 21st century. When using ±1 standard deviation to represent ICV, the ToE will move backwards by

around 10 years in particular for annual and wet season mean streamflows.

DISCUSSION

This study investigated the importance of ICV relative to HICC in hydrological climate change impact studies. To achieve this, a method to estimate the ToE of climate projections and hydrological simulations is proposed. This method estimates ICV based on the spread of a multi-member ensemble, and HICC based on the mean over multi-model projections together with that of a multi-member ensemble. A case study was conducted on the Hanjiang River watershed.

The results show that the ToE of mean temperature has already occurred during the end of the last century and the beginning of this century, but this is not the case for precipitation. Instead, for precipitation, the ToE is projected to occur around the 2050s, several decades later than for mean temperature. ICV for precipitation is large enough to obscure HICC for precipitation for the next few decades of the 21st century, until the constantly-increasing HICC becomes greater thereafter. With the joint contribution of temperature and precipitation, ToE of mean streamflow occurs about one decade later than that of precipitation, near the horizon of 2100. This is as expected, because the increase in temperature partly offsets the increase in streamflow resulting from precipitation increase through the increase in evapotranspiration.

The estimated ToE is dependent on how ICV and HICC are defined. In other words, different methods in estimating ICV and HICC may result in different ToEs. This study defined HICC as a multi-model ensemble mean. Even though some individual climate

model simulations may not be reliable in calculating the climate change signal, due to model uncertainty and climate variability, the multi-model ensemble mean can be considered as a more reliable solution, since the climate variability and model uncertainty are largely filtered out (Giorgi and Bi, 2009; Mahlstein et al., 2011; Maraun, 2013). When calculating the ensemble mean, all climate projections were considered equiprobable in this study. However, other studies (e.g. Giorgi and Mearns, 2002, 2003; Hawkins and Sutton, 2009) proposed that climate models should be weighted based on their ability to better represent various metrics over a reference period. Weighting climate model simulation is controversial when using multiple climate models for impact studies; and is especially so between climate modeling and impact assessment communities. However, a recent study (Chen et al., 2017) showed that weighting GCMs has a limited impact on projected future climate both in terms of precipitation and temperature changes and hydrological impacts.

The magnitude of HICC is also dependent on the greenhouse gas (GHG) emission scenario. Thus, the estimated ToE may also be sensitive to the GHG emission scenario, as has been pointed out in some studies (e.g. Giorgi and Bi, 2009). The magnitude of GHG-forced precipitation changes tends to become greater as the GHG forcing increases (Giorgi and Bi, 2009). The alternative scenarios for anthropogenic emissions give rise to changes in the ToE by a magnitude of a decade or more (Hawkins and Sutton, 2012). For example, warm scenarios tend to lead to earlier ToEs, while lower levels of emissions result not only in later ToEs, but also in a more gradual rise in temperature HICC, thus producing a large increase in the uncertainty of ToEs (Hawkins and Sutton,

2012). In order to make a conservative decision to counter climate change impacts, only one extreme GHG emission scenario is used to estimate HICC in this study.

ICV has been defined as the inter-member difference of a climate model. Since these ensemble members are projected within the same model structure and under the same forcing, inter-member difference can be considered as ICV. In other words, different ensemble members show how much climate can vary in the model world as a result of random internal variations. To the extent that the model simulates relevant physical processes, the range of ensemble provides insight into what could happen in the single realization that will occur in the real world (Deser et al., 2012a, 2012b). The same method has been used in several previous studies (e.g. Hulme et al., 1999; Deser et al., 2012a, 2012b; Fatichi et al., 2014). The results showed that multi-member ensemble of climate models can represent the observed ICV well at both regional and global scale. However, it should be noted that ICV is inherently complex and manifests itself over various temporal and spatial scales. This study only used multi-decadal variability to represent ICV at the multi-decadal scale. Multi-decadal variability is just one component of ICV, even though it is one of the key components for most climate change impact studies. Although some studies (e.g. Hawkins and Sutton, 2012; Maraun, 2013) defined the ToE as a specific year, the ToE estimated for a multi-year period may be more reliable and credible, since inter-annual variability is mostly filtered out by calculating multi-year averages. Moreover, climate change impact studies are commonly conducted at the multi-decadal time scale. For example, the classical period for estimating climate change is 30 years, as suggested by the World Meteorological

Organization (IPCC, 2014).

Other studies (e.g. Giorgi and Bi, 2009) defined the ToE as a time when HICC emerges from a combination of inter-model variability and natural variability (similar to ICV in this study). In other words, the noise of climate change was estimated based on ICV plus the inter-model variability. However, climate model uncertainty and ICV are different in origin, as ICV is a fundamental property of a climate system whilst model uncertainty is not (Hawkins and Sutton, 2012; Maraun, 2013). Moreover, consideration of ICV combined with model uncertainty is likely to give rise to a late warning of ToE, thus delaying detection and attribution for HICC. Therefore, it is more reasonable to use multi-member ensembles of climate models to estimate ICV, since climate model uncertainty plays a vital role in climate projection uncertainty (Jenkins and Lowe, 2003; Wilby and Harris, 2006; Chen et al., 2011a).

In addition, based on previous studies (e.g. Hulme et al., 1999; Mahlstein et al., 2011; Hansen et al., 2012; IPCC, 2013), ICV was defined as ±2 standard deviations of inter-member variability in this study. As justified by Hansen et al. (2012), it is commonly assumed that climate variability can be approximated as a normal distribution. A normal distribution of variability has only 68% of its climate change values falling within ±1 standard deviation of mean value. The tails of normal distribution decrease rapidly that there is only a 2.3% chance for climate change values to exceed 2 standard deviations. Therefore, ±2 standard deviations give a conservative criterion for detection of HICC. However, higher thresholds will cause later ToEs and lower thresholds will cause earlier ToEs. To date, the usage of the thresholds for ICV

estimation has not been exactly elucidated, a subject which deserves further studies.

This study only uses one hydrological model for hydrological simulations. However, the hydrological model itself is one of uncertainty sources for climate change impact studies. Thus, it may be necessary to consider hydrological model uncertainty in estimating the importance of ICV in climate change impact studies. On the other hand, previous studies (e.g. Wilby and Harris, 2006; Chen et al., 2011a) also showed that climate model uncertainty is more significant than the uncertainty related to hydrological models.

CONCLUSION

This study investigated the importance of ICV relative to HICC in hydrological climate change impact studies, using a multi-member ensemble of a climate model for the Hanjiang River watershed. The following conclusions are drawn:

1. The ToE of temperature has already occurred at around the end of the last century. However, the ToE of precipitation is projected to happen in the middle of the 21st century, much later than the ToE for temperature.
2. For mean streamflow, the ToE is projected to happen around the end of the 21st century, later in wet season than in dry season. In other words, ICV is likely to have greater importance on climate change hydrological impacts in this century for the Hanjiang River watershed.
3. Overall, in the near future, ICV is still the main cause of hydrological variability for the Hanjiang River watershed, and HICC is mostly obscured by ICV. However, as

the anthropogenic forcing (e.g. greenhouse gas emissions) increases, HICC will contribute more and more to hydrological changes.

4. The results of this study imply that adapting to ICV may well turn out to be the most efficient approach in the near future, but in the long-term future, more attention should be paid to HICC.

Acknowledgements

This work was partially supported by the National Key Research and Development Program of China (Grant No. 2017YFA0603704), the National Natural Science Foundation of China (Grant No. 51779176, 51525902, 51539009) and the Thousand Youth Talents Plan from the Organization Department of the CCP Central Committee (Wuhan University, China). The authors would like to acknowledge the contribution of the World Climate Research Program Working Group on Coupled Modelling, and of climate modeling groups for making available their respective climate model outputs. The authors wish to thank the China Meteorological Data Sharing Service System and the Bureau of Hydrology of the Changjiang Water Resources Commission for providing datasets for the Hanjiang River watershed.

References

Arsenault, R., Poulin, A., Côté, P. & Brissette, F. 2013 Comparison of stochastic optimization algorithms in hydrological model calibration. *Journal of Hydrologic Engineering*, 19(7), 1374-1384.

Chen, H., Guo, S.L., Xu, C-Y. & Singh, V.P. 2007 Historical temporal trends of hydro-climatic variables and runoff response to climate variability and their relevance in water resource management in the Hanjiang basin. *Journal of Hydrology*, 344, 171-184.

Chen, H., Xu, C-Y. & Guo, S.L. 2012 Comparison and evaluation of multiple GCMs, statistical downscaling and hydrological models in the study of climate change impacts on runoff. *Journal of Hydrology*, 434-435, 36-45.

Chen, J., Brissette, F. P., Chaumont, D. & Braun, M. 2013 Performance and uncertainty evaluation of empirical downscaling methods in quantifying the climate change impacts on hydrology over two North American river basins. *Journal of Hydrology*, 479, 200-214.

Chen, J., Brissette, F. P. & Leconte, R. 2011b Uncertainty of downscaling method in quantifying the impact of climate change on hydrology. *Journal of Hydrology*, 401, 190–202.

Chen, J., Brissette, F. P., Lucas-Picher, P. & Caya, D. 2017 Impacts of weighting climate models for hydro-meteorological climate change studies. *Journal of Hydrology*, 549, 534-546.

Chen, J., Brissette, F. P., Poulin, A. & Leconte, R. 2011a Overall uncertainty study of the hydrological impacts of climate change for a Canadian watershed. *Water Resources Research*, **47**(12), W12509.

Chen, J., Zhang, X. J. & Brissette, F. P. 2014 Assessing scale effects for statistically downscaling precipitation with GPCC model. *International Journal of Climatology*, **34**(3), 708-727.

Chow, V.T., Maidment, D.R. & Mays, L.W. 1988 Applied Hydrology. *Tata McGraw-Hill Education, New York, USA*.

Dai, A., Fyfe, J. C., Xie, S. P. & Dai, X. 2015 Decadal modulation of global surface temperature by internal climate variability. *Nature Climate Change*, **5**(6), 555-559.

Deng, C., Liu, P., Liu, Y., Wu, Z. & Wang, D. 2014 Integrated hydrologic and reservoir routing model for real-time water level forecasts. *Journal of Hydrologic Engineering*, 20(9), 05014032.

Deser, C., Knutti, R., Solomon, S. & Phillips, A. S. 2012b Communication of the role of natural variability in future North American climate. *Nature Climate Change*, **2**(11), 775-779.

Deser, C., Phillips, A. S., Alexander, M. A. & Smoliak, B. V. 2014 Projecting North American climate over the next 50 years: uncertainty due to internal variability*. *Journal of Climate*, **27**(6), 2271-2296.

Deser, C., Phillips, A. S., Bourdette, V. & Teng, H. 2012a Uncertainty in climate change projections: the role of internal variability. *Climate Dynamics*, **38**(3-4), 527-546.

Fasullo, J. T. & Nerem, R. S. 2016 Interannual variability in global mean sea level estimated from the CESM Large and last millennium ensembles. *Water*, 8(11), 491.

Fatichi, S., Rimkus, S., Burlando, P. & Bordoy, R. 2014 Does internal climate variability overwhelm climate change signals in streamflow? The upper Po and Rhone basin case studies. *Science of the Total Environment*, 493, 1171-1182.

Fenton, J.D. 1992 Reservoir routing. *Hydrological Sciences Journal*, 37(3), 233-246.

Fyfe, J. C., Gillett, N. P. & Zwiers, F. W. 2013 Overestimated global warming over the past 20 years. *Nature Climate Change*, **3**(9), 767-769.

Fyfe, J. C., Meehl, G. A., England, M. H., Mann, M. E., Santer, B. D., Flato, G. M., Hawkins, E., Gillett, N. P., Xie, S. P., Kosaka, Y. & Swart, N. C. 2016 Making sense of the early-2000s warming slowdown. *Nature Climate Change*, **6**(3), 224-228.

Giorgi, F. & Bi, X. 2009 Time of emergence (TOE) of GHG‐forced precipitation change hot‐spots. *Geophysical Research Letters*, **36**(6), L06709.

Giorgi, F. & Mearns, L.O., 2002 Calculation of average, uncertainty range, and reliability of regional climate changes from AOGCM simulations via the "reliability ensemble averaging" (REA) method. *Journal of Climate*, 15, 1141–1158.

Giorgi, F. & Mearns, L.O., 2003 Probability of regional climate change based on the reliability ensemble averaging (REA) method. *Geophysical Research Letters*, 30, 1629.

Hansen, J., Sato, M. & Ruedy, R. 2012 Perception of climate change. *Proceedings of the National Academy of Sciences*, 109(37), E2415-E2423.

Hansen, N. & Ostermeier, A. 2001 Completely derandomized self-adaptation in evolution strategies. *Evolutionary computation*, **9**(2), 159-195.

Hawkins, E. & Sutton, R. 2009 The potential to narrow uncertainty in regional climate predictions. *Bulletin of the American Meteorological Society*, **90**(8), 1095-1107.

Hawkins, E. & Sutton, R. 2011 The potential to narrow uncertainty in projections of regional precipitation change. *Climate Dynamics*, **37**(1-2), 407-418.

Hawkins, E. & Sutton, R. 2012 Time of emergence of climate signals. *Geophysical Research Letters*, **39**(1), L01702.

Helama, S., Fauria, M. M., Mielikäinen, K., Timonen, M. & Eronen, M. 2010 Sub-Milankovitch solar forcing of past climates: mid and late Holocene perspectives. *Geological Society of America Bulletin*, 122(11-12), 1981-1988.

Hu, A. & Deser, C. 2013 Uncertainty in future regional sea level rise due to internal climate variability. *Geophysical Research Letters*, 40(11), 2768–2772.

Hulme, M., Barrow, E. M., Arnell, N. W., Harrison, P. A., Johns, T. C. & Downing, T. E. 1999 Relative impacts of human-induced climate change and natural climate variability. *Nature*, **397**(6721), 688-691.

Jenkins, G. & Lowe, J. 2003 Handling uncertainties in the UKCIP02 scenarios of climate change. *Hadley Centre, Technical note 44, Exeter, UK*.

Kang, S. M., Deser, C. & Polvani, L. M. 2013 Uncertainty in climate change projections of the Hadley circulation: The role of internal variability. *Journal of Climate*, 26, 7541-7554.

Kay, J. E., Deser, C., Phillips, A., Mai, A., Hannay, C., Strand, G., Arblaster, J. M., Bates, S. C., Danabasoglu, G., Edwards, J., Holland, M., Kushner, P., Lamarque, J. –F., Lawrence, D., Lindsay, K., Middleton, A., Munoz, E., Neale, R., Oleson, K., Polvani, L. & Vertenstein, M. 2015 The Community Earth System Model (CESM) large ensemble project: A community resource for studying climate change in the presence of internal climate variability. *Bulletin of the American Meteorological Society*, **96**(8), 1333-1349.

Leng, G., Huang, M., Voisin, N., Zhang, X., Asrar, G. R. & Leung, L. R. 2016 Emergence of new hydrologic regimes of surface water resources in the conterminous United States under future warming. *Environmental Research Letters*, 11(11), 114003.

Lu, J., Hu, A. & Zeng, Z. 2014 On the possible interaction between internal climate variability

and forced climate change. *Geophysical Research Letters*, 41(8), 2962-2970.

Mahlstein, I., Knutti, R., Solomon, S. & Portmann, R. W. 2011 Early onset of significant local warming in low latitude countries. *Environmental Research Letters*, **6**(3), 034009.

Maraun, D. 2013 When will trends in European mean and heavy daily precipitation emerge?, *Environmental Research Letters*, 8(1), 014004.

Martel, J.-L., Demeester, K., Brissette, F.P., Poulin, A. & Arsenault, R. 2017 HMETS - A simple and efficient hydrology model for teaching hydrological modelling, flow forecasting and climate change impacts. *International Journal of Engineering Education*, 33(4), 1307-1316.

Mpelasoka, F.S. & Chiew, F.H.S. 2009 Influence of rainfall scenario construction methods on runoff projections. *Journal of Hydrometeorology*, 10 (2009), pp. 1168-1183.

Otto-Bliesner, B. L., Brady, E. C., Fasullo, J., Jahn, A., Landrum, L., Stevenson, S., Rosenbloom, N., Mai, A. & Strand, G. 2015 Climate variability and change since 850 c.e.: an ensemble approach with the community earth system model (cesm). *Bulletin of the American Meteorological Society*, 97(5), 150807114607005.

Pachauri, R. K., Meyer, L., Plattner, G. K. & Stocker, T. 2014 IPCC, 2014. Climate change 2014. The Physical Science Basis. Contribution of Working Group I, II and III to the Fifth Assessment Report of the Intergovernmental Panel on Climate Change. *Cambridge University Press, Cambridge, United Kingdom and New York, NY, USA*, pp. 996.

Ricke, K. L. & Caldeira, K. 2014 Natural climate variability and future climate policy. *Nature Climate Change*, 4(5), 333-338.

Schmidli, J., Frei, C. & Vidale, P. L. 2006 Downscaling from GCM precipitation: A benchmark for dynamical and statistical downscaling methods. *International journal of climatology*, 26, 679–689.

Stocker, T. F., Qin, D., Plattner, G.-K., Tignor, M., Allen, S. K., Boschung, J., Nauels, A., Xia, Y., Bex, V. & Midgley, P. M. 2013 IPCC, 2013. Climate change 2013. The Physical Science Basis. Contribution of Working Group I to the Fifth Assessment Report of the Intergovernmental Panel on Climate Change. *Cambridge University Press, Cambridge, United Kingdom and New York, NY, USA*, pp. 996.

Swart, N. C., Fyfe, J. C., Hawkins, E., Kay, J. E. & Jahn, A. 2015 Influence of internal variability on Arctic sea-ice trends. *Nature Climate Change*, **5**(2), 86-89.

Wang, L., Huang, C. C., Pang, J., Zha, X. & Zhou, Y. 2014 Paleofloods recorded by slackwater deposits in the upper reaches of the Hanjiang River valley, middle Yangtze River basin, China. *Journal of Hydrology*, **519**, 1249-1256.

Wang, Y., Wang, D. & Wu, J. 2015 Assessing the impact of Danjiangkou reservoir on ecohydrological conditions in Hanjiang river, China. *Ecological Engineering*, **81**, 41-52.

Wilby, R. L. & Harris, I. 2006 A framework for assessing uncertainties in climate change impacts: Low - flow scenarios for the River Thames, UK. *Water Resources Research*, **42**(2), W02419.

Xu, Y. P., Yu, C., Zhang, X., Zhang, Q. & Xu, X. 2012 Design rainfall depth estimation through two regional frequency analysis methods in Hanjiang River Basin, China. *Theoretical and Applied Climatology*, **107**(3-4), 563-578.

Yang, G., Guo, S., Li, L., Hong, X. & Wang, L. 2016 Multi-objective operating rules for danjiangkou reservoir under climate change. *Water Resources Management*, 30(3), 1183-

1202.

Yang, H. & Zehnder, A.J.B. 2005 The south–north water transfer project in China – an analysis of water demand uncertainty and environmental objectives in decision making. *Water International*, 30 (3), 339–349.

Table

Table 1 General information of 30 GCMs used

Modeling center	Institution	Model name	Horizontal resolution (lon. x Lat.)	ID
CSIRO-BOM	CSIRO (Commonwealth Scientific and Industrial Research Organisation Australia), and BOM (Bureau of Meteorology, Australia)	ACCESS1.0	1.875 x 1.25	**1**
		ACCESS1.3	1.875 x 1.25	**2**
BCC	Beijing Climate Center, China Meteorological Administration	BCC-CSM1.1	2.8 x 2.8	**3**
		BCC-CSM1.1(m)	1.125 x 1.125	**4**
GCESS	College of Global Change and Earth System Science, Beijing Normal University	BNU-ESM	2.8 x 2.8	**5**
CCCma	Canadian Centre for Climate Modelling and Analysis	CanESM2	2.8 x 2.8	**6**
		CESM1-CAM5	1.25 x 0.9	**7**
NCAR	National Center for Atmospheric Research	CESM1	1.25 x 0.9	**8**
CMCC	Centro Euro-Mediterraneo per I Cambiamenti Climatici	CMCC-CESM	3.75 x 3.7	**9**
		CMCC-CM	0.75 x 0.7	**10**
		CMCC-CMS	1.875 x 1.875	**11**
CNRM-CERFACS	Centre National de Recherches Meteorologiques/Centre Europeen de Recherche et Formation Avancees en Calcul Scientifique	CNRM-CM5	1.4 x 1.4	**12**
CSIRO-QCCCE	Commonwealth Scientific and Industrial Research Organisation in collaboration with the Queensland Climate Change Centre of Excellence	CSIRO-Mk3.6.0	1.875 x 1.875	**13**
ICHEC	Irish Centre for High-End Computing	EC-EARTH	1.1x 1.1	**14**
LASG-CESS	LASG, Institute of Atmospheric Physics, Chinese Academy of Sciences; and CESS, Tsinghua University	FGOALS-g2	1.875 x 1.25	**15**
NOAA-GFDL	Geophysical Fluid Dynamics Laboratory	GFDL-CM3	2.5 x 2.0	**16**
		GFDL-ESM2G	2.5 x 2.0	**17**
		GFDL-ESM2M	2.5 x 2.0	**18**
NIMR-KMA	National Institute of Meteorological Research	HadGEM2-AO	1.875 x 1.25	**19**
MOHC	Met Office Hadley Centre	HadGEM2-CC	1.875 x 1.25	**20**
		HadGEM2-ES	1.875 x 1.25	**21**
INM	Institute for Numerical Mathematics	INM-CM4	2.0 x 1.5	**22**
IPSL	Institut Pierre-Simon Laplace	IPSL-CM5A-LR	3.75 x 1.875	**23**
		IPSL-CM5A-MR	2.5 x 1.25	**24**
		IPSL-CM5B-LR	3.75 x 1.875	**25**
MPI-M	Max Planck Institute for Meteorology	MPI-ESM-LR	1.875 x 1.8	**26**
		MPI-ESM-MR	1.875 x 1.8	**27**
MRI	Meteorological Research Institute	MRI-CGCM3	1.125 x 1.125	**28**
		MRI-ESM1	1.1 x 1.1	**29**
NCC	Norwegian Climate Centre	NorESM1-M	2.5 x 1.9	**30**

Figure Lists

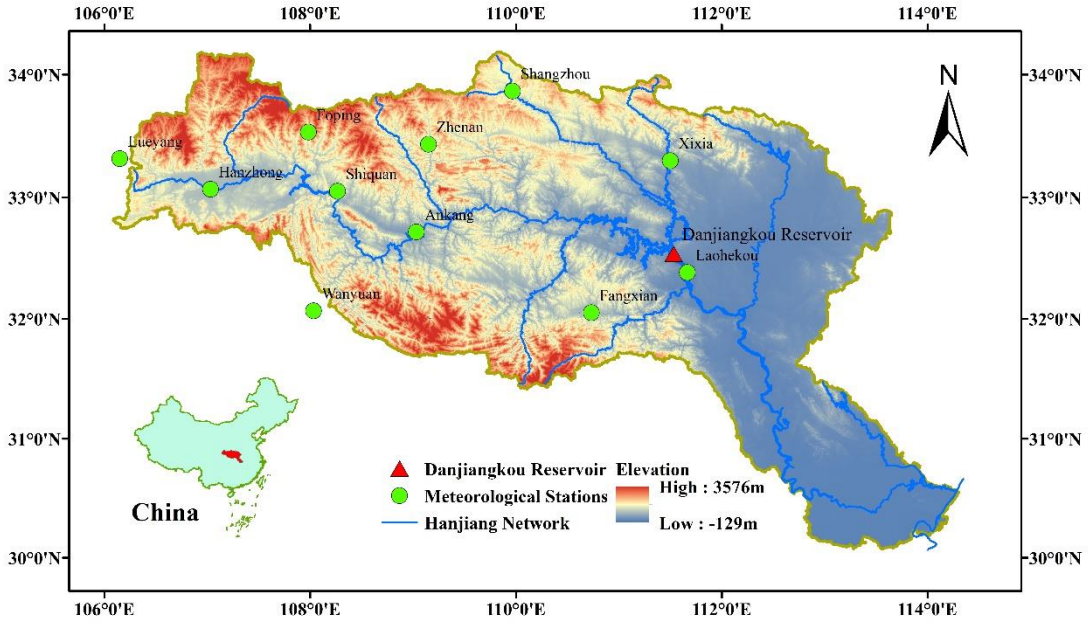

Figure 1. Location of the Hanjiang River watershed.

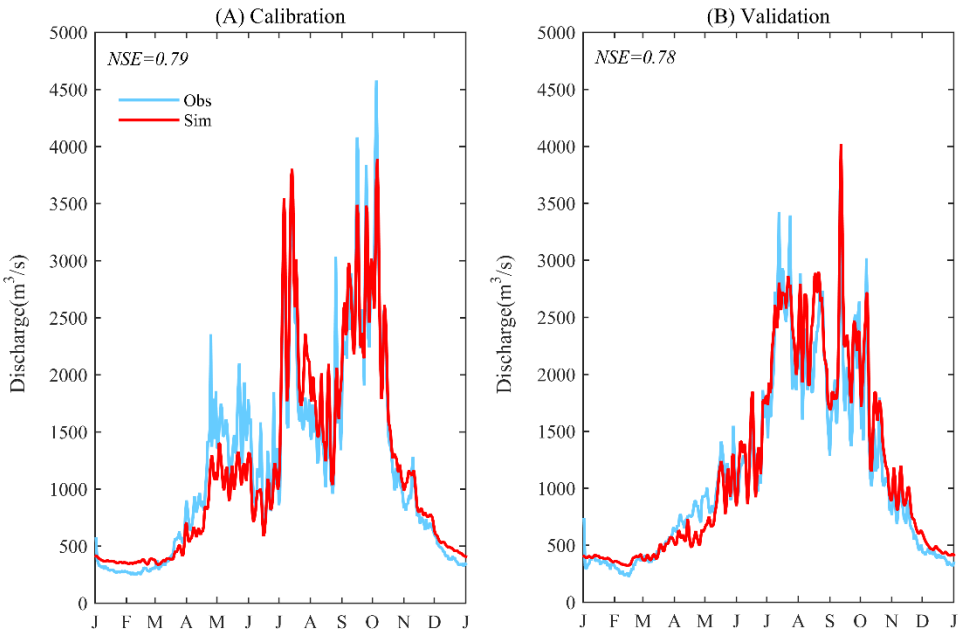

Figure 2. Observed and HMETS-simulated mean hydrographs for (A) calibration (1961-1980) and (B) validation (1981-2000) periods for the Hanjiang River watershed.

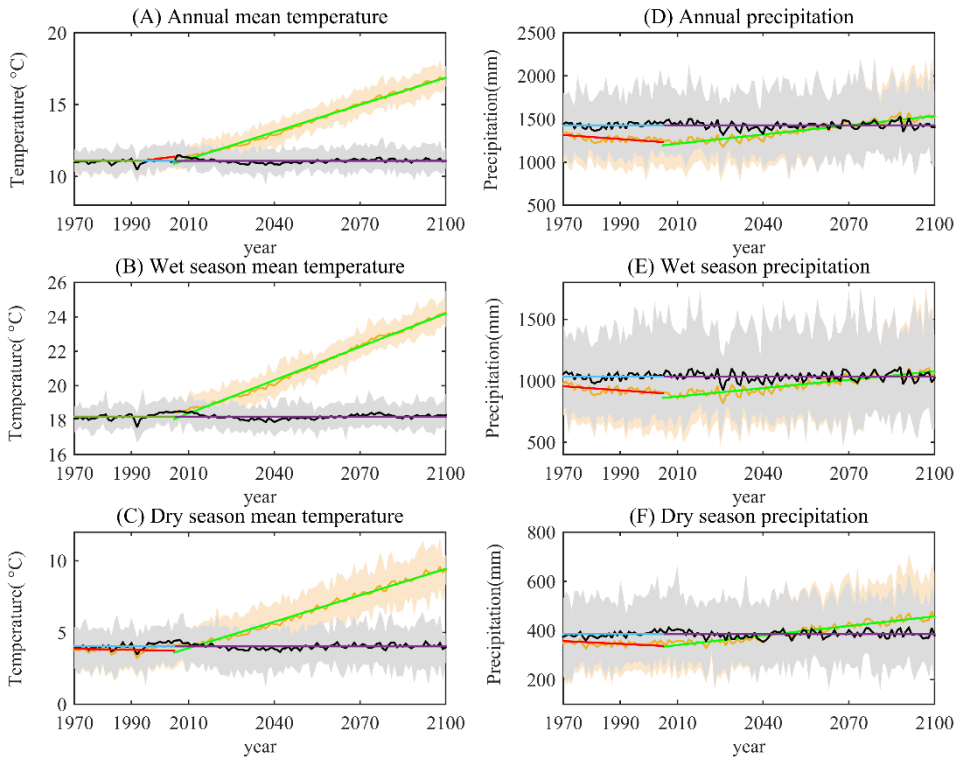

Figure 3. Raw and detrended CESM1 (A-C) mean temperature and (D-F) precipitation time series at annual and seasonal time scales, respectively, over the 1970-2100 period in the Hanjiang River watershed.

Note: grey and orange shades show the ranges of precipitation or temperature ensembles with and without detrending, respectively. The orange and black curves show the ensemble means for non-detrended and detrended data, respectively. Red and bright green lines are the best-fit linear trends to the orange curves for the second historical sub-period and the future period, respectively.

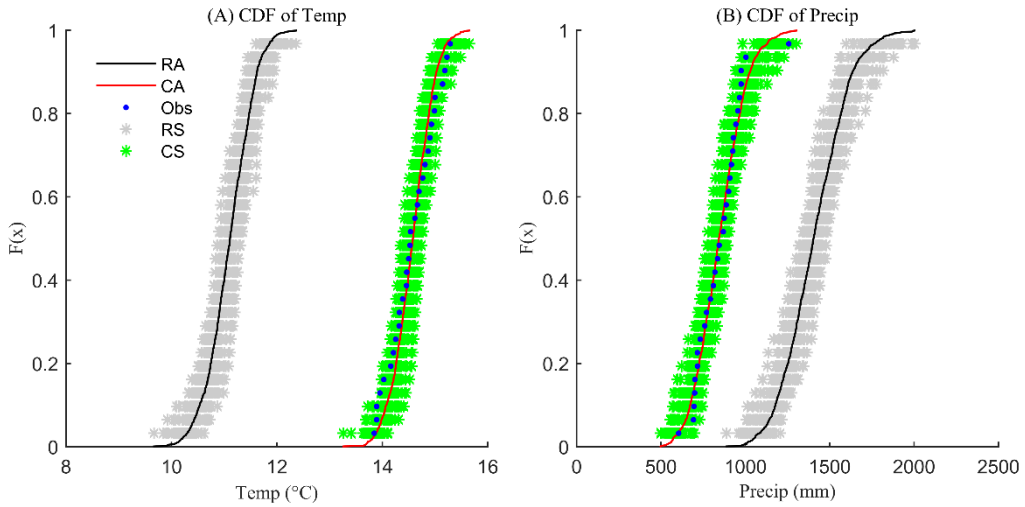

Figure 4. Empirical cumulative distribution functions (CDFs) for annual (A) mean temperature and (B) precipitation. (RA: all raw 40 members; CA: all corrected 40 members; Obs: observed data; RS: each of the raw 40 members and the green symbols represent the spread of the 40 ensemble members; CS: each of the corrected 40 members and the gray symbols represent the spread of the 40 ensemble members).

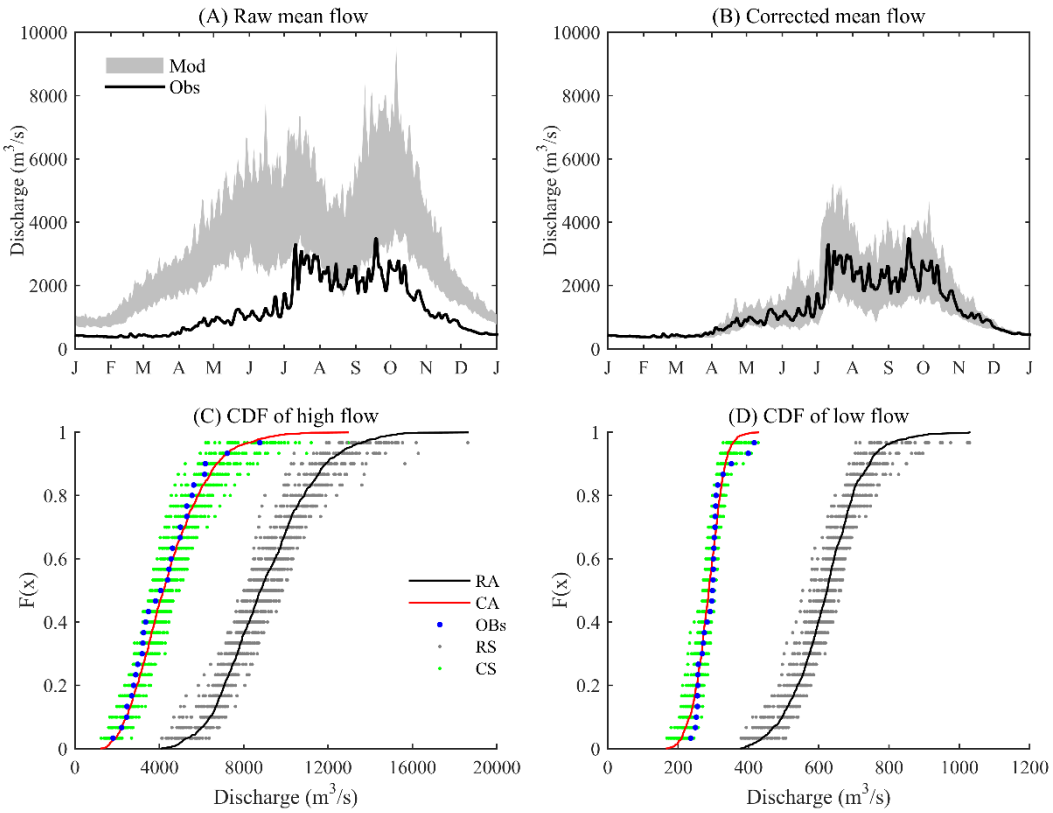

Figure 5. Mean hydrographs simulated by (A) raw and (B) corrected climate data for reference period (1971-2000) and empirical cumulative distribution functions (CDFs) of (C) annual 95th percentile high flow and (D) annual 5th percentile low flow for the same period. (Mod: hydrographs of ensemble; Obs: hydrograph of observed data; RA: all raw 40 members of annual flows; CA: all corrected 40 members of annual flows; OBs: observed data of annual flows; RS: each of the raw 40 members and the green symbols represent the spread of the 40 ensemble members; CS: each of the corrected 40 members and the gray symbols represent the spread of the 40 ensemble members).

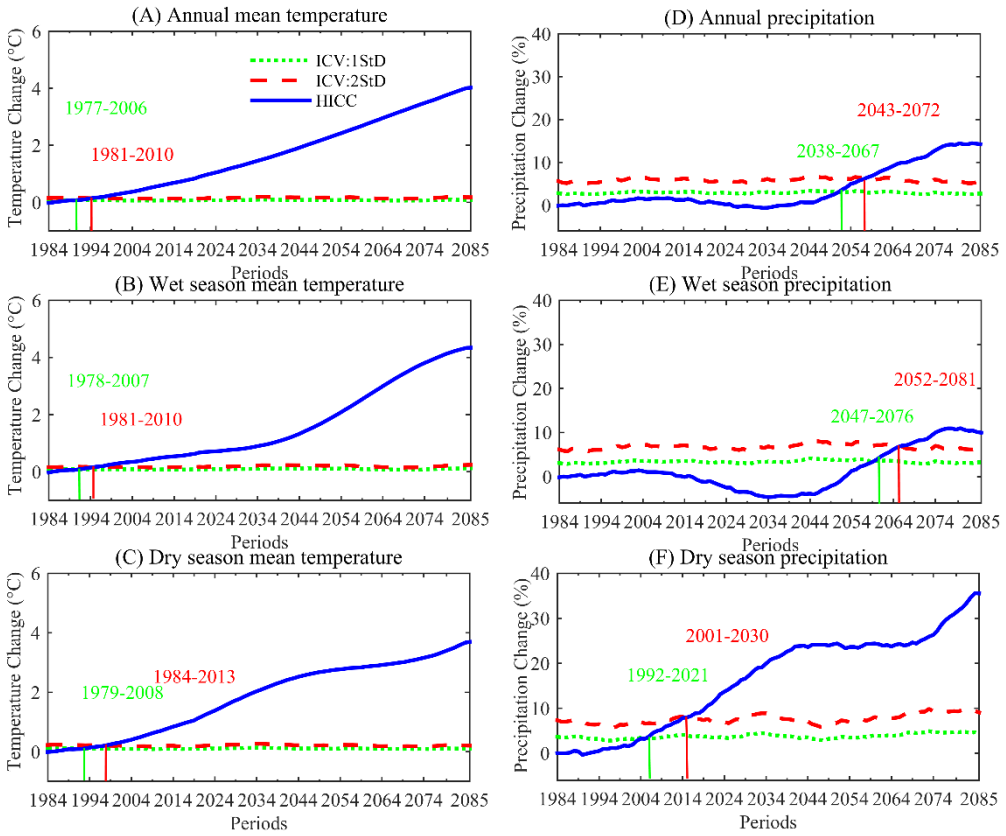

Figure 6. ToEs for annual and seasonal (A-C) mean temperatures and (D-F) precipitations in the Hanjiang River watershed. (Green dot lines: ICV estimated as 1 standard deviation of inter-member differences; red dash lines: ICV estimated as 2 standard deviations of inter-member differences; blue solid lines: human-induced climate change).

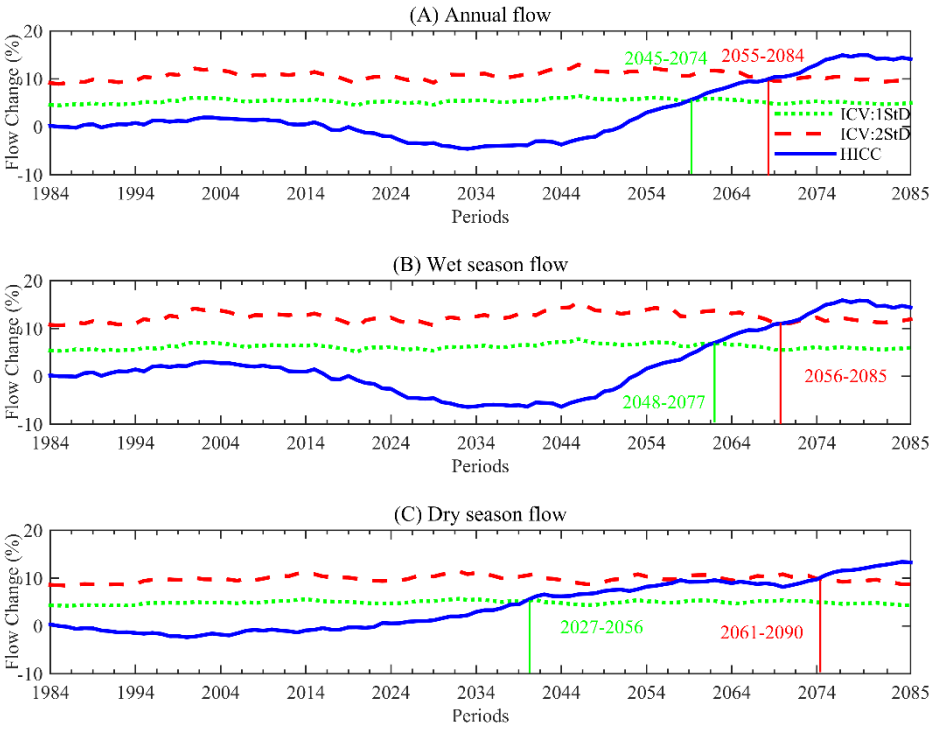

Figure 7. ToEs for annual and seasonal mean streamflows in the Hanjiang River watershed. (Green dot lines: ICV estimated as 1 standard deviation of inter-member differences; red dash lines: ICV estimated as 2 standard deviations of inter-member differences; blue solid lines: human-induced climate change).